PRESTRESSED CFRP STRIPS FOR CONCRETE BRIDGE GIRDER RETROFITTING - APPLICATION AND STATIC LOADING TEST

Julien Michels[1], Michał Staśkiewicz[2], Christoph Czaderski[3], Renata Kotynia[4], Yunus Emre Harmanc

Masoud Motavalli[6], Member, ASCE

ABSTRACT

This paper presents an investigation on the practicability and structural efficiency of prestressed CFRP strips with a gradient anchorage in the framework of a bridge

[1]PhD, Project Leader, Empa, Swiss Federal Laboratories for Materials Science and Technology, Structural Engineering Research Laboratory, Überlandstrasse 129, CH-8600 Dübendorf, Switzerland. E-mail: julien.michels@empa.ch

[2]MSc, PhD candidate, Łódź University of Technology, Department of Concrete Structures, 90-924 Łódź, Poland. Email: michal.staskiewicz@p.lodz.pl

[3]PhD, Senior Scientist, Empa, Swiss Federal Laboratories for Materials Science and Technology, Structural Engineering Research Laboratory, Überlandstrasse 129, CH-8600 Dübendorf, Switzerland. E-mail: christoph.czaderski@empa.ch

[4]PhD, Associate Professor, Łódź University of Technology, Department of Concrete Structures, 90-924 Łódź, Poland. Email: renata.kotynia@p.lodz.pl

[5]MSc, Research Assistant, ETHZ, Swiss Federal Institute of Technology Zurich, Institute of Structural Engineering, Stefano-Franscini-Platz 5, CH-8093 Zürich / Empa, Swiss Federal Laboratories for Materials Science and Technology, Structural Engineering Research Laboratory, Überlandstrasse 129, CH-8600 Dübendorf, Switzerland. E-mail: harmanci@ibk.baug.ethz.ch

[6]PhD, Professor, Laboratory Head, Empa, Swiss Federal Laboratories for Materials Science and Technology, Structural Engineering Research Laboratory, Überlandstrasse 129, CH-8600 Dübendorf, Switzerland. E-mail: masoud.motavalli@empa.ch

strengthening application in Poland. The non-mechanical anchorage system avoids the installation of metallic bolts and plates, with the exception of a temporary support frame. Two 18.4 m long large-scale prestressed concrete girders were produced following the drawings of the existing bridge construction. One girder served as reference, the second one was strengthened with two prestressed Carbon Fiber Reinforced Polymer (CFRP) strips. In this case, the initial negative cambering was levelled out by a layer of dry shotcrete. CFRP strips with a prestrain of 0.58% were applied for flexural upgrading. Both girders with a total length of 18.4 m were finally statically loaded up to failure in order to assess the strengthening efficiency in flexure of the used retrofitting technique. It was shown that tensile failure of the CFRP strips was reached, indicating an optimal use of the composite reinforcement. The strengthened girder exhibited a ductile behavior up to strip rupture with a distinct steel yielding and a subsequent pronounced increase of the load carrying capacity. For service load considerations, an enhancement of the cracking load of about 16% was noticed. In terms of ultimate load, a significant improvement of about 25% compared to the reference girder was reached. Although some practical problems need optimization, the presented results are very promising and make this strengthening system an alternative for future retrofitting applications in bridge engineering.

Keywords: Prestressed concrete bridge girder, flexural and shear strengthening, prestressed CFRP strips, dry shotcrete, static testing

BACKGROUND

The application of Carbon Fiber Reinforced Polymer (CFRP) strips in structural strengthening is nowadays well accepted (Meier 1995),(Bakis et al. 2002).

Their use in the civil engineering domain has drastically increased over the last three decades, several available design codes and recommendations (see (fib bulletin14 2001),(ACI440.2R-8 2008),(SIA166 2004),(DAfStb 2012), among others) attest their popularity. Applications with initially unstressed CFRP strips as an externally bonded (EBR) or near-surface mounted (NSM) technique in bridge engineering can be found (Blaschko and Zehetmaier 2008),(Petrou et al. 2008),(Bae and Belarbi 2013),(Cerullo et al. 2013),(Kasan et al. 2014). An on-site failure test of a CFRP-strengthened railway concrete bridge is for instance presented by (Puurula et al. 2014). Strengthening with prestressed CFRP laminates, however, have surprisingly not known a similar success, despite the undeniable advantages such as reduction of crack widths, reduction of deflections as well as increased cracking, yielding, and ultimate load (El-Hacha et al. 2001),(Wight et al. 2001),(Pellegrino and Modena 2009),(Michels et al. 2013). Moreover, the strip prestressing usually involves a much more efficient use of the composite's excellent mechanical properties, mainly the high tensile strength. Whereas in case of an initially unstressed strip failure generally occurs by strip debonding at strain levels below 1.0%, an initial prestrain can shift the maximum strains close to tensile failure (Meier and Stöcklin 2005),(Suter and Jungo 2001),(Kotynia et al. 2011). A key factor in prestressing is the anchorage system. Nowadays, most available solutions (commercially available and at laboratory level) are so-called 'mechanical' systems, which utilize mechanical plates and bolts at the strips ends to avoid debonding (Berset et al. 2002),(El-Hacha et al. 2003),(Pellegrino and Modena 2009),(Xue et al. 2008). One example of the few applications of prestressed CFRP sheets in a bridge retrofitting project is given in (Kim et al. 2008).

The *gradient anchorage* applies a gradual prestress force release with intermediate accelerated adhesive curing at both strips ends until no pressure remains in the hydraulic system. It is based on the epoxy resin's ability to develop strength and stiffness faster under high temperatures (Czaderski et al. 2012). Early research is documented in (Meier et al. 2001), (Kotynia et al. 2011), and (Michels et al. 2013).

The final step was the flexural upgrading of a road bridge in Szczercowska Wieś (Poland, see Figure 1).The bridge was built in the 1960s and is composed of five simply supported simple span prestressed concrete (PC) girders and a reinforced concrete (RC) deck. The girders were precast and delivered to the construction site, the plate was cast on-site. In the framework of the strengthening project in 2014, the upper deck was replaced by a thicker plate. The current cross-section of the old bridge is given in Figure 2. Each girder was prestressed with three parabolic cables and two straight cables in the bottom flange (see Figure 3). The two principal aims of this investigation are: 1) verify the practicability of the technique in such a bridge strengthening case, and 2) assess the structural efficiency when two prestressed CFRP strips with a gradient anchorage are used for flexural upgrading of one girder. For this purpose, two girders have been reproduced according to the original drawings and subsequently tested under static loading. Whereas one served as reference, the second one was strengthened with two prestressed CFRP strips with gradient anchorage prior to testing. Additionally a shear reinforcement in compliance with the Polish Standard (PN-91/S-10042 1991) was applied in the form of CFRP wraps. This paper will present the girder production, the different strengthening steps as well as the final static tests and the related results.

GIRDER FABRICATION

This section briefly summarizes key material characteristics and explains the different production and prestressing steps.

Materials and girder production

Due to the slender geometry of the girders, a self-compacting concrete C35/45 with a maximum aggregate size d_{max} of 16 mm was chosen for casting. The upper slabs were casted with a regular C30/37 with a maximum aggregate size of 16 mm and a w/c ratio of 0.49. Compressive strength f_{cm}, tested on 150·150·150 mm^3 cubes, and elastic modulus E_{cm}, tested on 120·120·360 mm^3 prisms, are given at 28 days and at the testing day in Table 1.

Yield strength, ultimate tensile strength as well as strain at failure of the reinforcing steel bars with a diameter Ø of 6 and 8 mm are summarized in Table 2. It is mentioned that for a structural assessment as realistic as possible, the passive steel reinforcement had no ribs.

Prestressing tendons had a total cross-section A_p of 345 mm^2. The average yield limit $R_{p,0.1}$ at 0.1% strain was about 1660 MPa and the average ultimate strength R_m was approximately 1810 MPa according to the testing certificate provided by the distributor. Average elastic modulus E_{nom} was 201.3 GPa, and average strain at failure A_g was 3.76%.

A photo of the formwork as well as the the girder casting is given in Figure 4. The steel bars in the bridge girders are smooth without any ribs. After casting, the second fabrication step comprises the prestressing of three parabolic and two straight steel tendons. Each tendon was prestressed to an initial prestressing force $F_{fp,0}$ of about 363 kN. Initial negative cambers at midspan of about 33 mm were measured for Girder 1 and 2. Calculated compression stress on the bottom fiber was in this case 28 MPa, a bit below 50% of the compressive strength. For the weeks following the prestressing application, creep behavior was monitored. Figure 5 presents the evolution of the negative deflection at the girder midspan. Lastly, a part of the new upper concrete deck with a width of 125 cm and a thickness of 21 cm was casted. The complete cross-section in shown in Figure 6.

For flexural strengthening, a commercially available two-component epoxy resin was used. The CFRP strips had a width b_f of 100 mm and a thickness of t_f of 1.2 mm. According to the distributor, the strips have a nominal elastic modulus E_f of 165 GPa, later on used for deriving the total prestressing force from the measured prestrain. Tensile tests on small strip specimens have been performed according to (DIN-EN-ISO-527-5 1997) and revealed a undirectional tensile strength $f_{f,u}$ of 2795 (+/-115) MPa at an average failure strain of 1.6%. CFRP wraps with an elastic modulus E_f above 240 GPa and a strain at failure $\varepsilon_{f,u}$ of 1.7 % were installed as shear reinforcement. These and several other characteristics can be taken from the referenced data sheet.

Surface levelling

The surface levelling procedure was chosen according to a preceded experimental investigation on the bond behavior of CFRP strips with various cementitious subtrates (Michels et al. 2014). Prior to the shotcrete application, the bottom surface of the girder was roughened by high-pressure waterjetting, see Figure 7 (top). Subsequently, dry shotcrete with a maximum aggregate diameter d_{max} of 8 mm and a guaranteed compressive strength of 60 MPa after 28 days was applied. The application, for which the girder was covered with a plastic plane for protection against the strong rebound and dust formation, is presented in Figure 7 (bottom). On the day of the shotcrete application, which took place more than a year after the last reading on Figure 5, the maximum camber level at midspan was about 60 mm.

Flexural strengthening

Each CFRP strip was prestressed to a strain level $\varepsilon_{fp,0}$ of 0.58%, which corresponds to a prestressing force $F_{fp,0}$ of about 115 kN, calculated with the previously indicated elastic modulus of 165 GPa. Since two strips are applied, additional 230 kN are introduced in the girder cross-section. The gradient anchorage at the strip ends was realized by following the identical program as described in (Michels et al. 2013), i.e. three consecutive force releases ΔF of 50, 35, and 35 kN over 300, 200 and 200 mm bond lengths, respectively. In terms of prestressing technique, a *prestressing against the structure* (El-Hacha et al. 2001) was applied. Due to the slender geometry and the inner prestressing steel tendons, no drilling to the girder was allowed and thus a temporary steel frame, responsible for the force transfer to the girder during the prestressing, was mounted by adhesive bonding. Despite an initial debonding of the first CFRP strip during the installation (which involved the necessity of repeating the procedure), it was eventually possible to anchor both laminates at the desired prestrain level. During the releasing of the second CFRP strip, a large crack appeared in the anchorage zone without however inducing a debonding failure. The strain level in the CFRP strip remained constant. The crack was afterwards injected with a resin and had, as shown later in the paper, no effect on the load carrying capacity of the girder. An adapted procedure was followed for the final bridge application. A photo of the girder bottom side with two strips is shown in Figure 8.

Shear strengthening

The fabric had an initial width b_f of 30 cm and was folded twice to obtain a final width of about 7.5 cm, the final wrap thickness t_f is approximately 1 mm. They were subsequently bonded to the concrete by wet-lay-up procedure around the total cross section to include the compression zone (Figure 8). Prior to the application, concrete filling elements were installed to dispose of a regular cross-section geometry at the respective locations.

CROSS SECTION ANALYSIS (CSA)

Flexural resistance was evaluated by means of a cross-section analysis (CSA) (see Figure 9). The complex girder geometry due to the curved inner prestress cables and the related variable cable position d_p along the horizontal girder axis implicates that the force equilibrium and strain compatibility have to be established on several locations along the girder in order to derive the curvature χ and finally by double integration the deflection δ at midspan (Harmanci 2013). Strength values are considered as indicated in the 'Materials' section. Steel reinforcements (passive and prestressed) were considered with bi-linear constitutive laws, including a stiffening behavior up to failure after reaching the yield stress (see Table 2). CFRP strips were considered as perfectly linear elastic up to failure. Finally, concrete was included as linear elastic in tension until reaching tensile strength f_{ct}, in compression a second-degree parabola was implemented (Hognestad 1951),(Park and Paulay 1975). For both the prestress steel cables and the CFRP reinforcement, prestressing was included as a prestrain at the moment of the first loading. In Figure 9, the example of the strain state after prestressing and anchoring the CFRP strip is shown. The initial strip prestrain $\varepsilon_{fp,0}$ increases due to the ongoing static loading by $\Delta\varepsilon_f$, resulting in a total strip strain ε_f. The total concrete compressive strain corresponds to ε_c, the total cable stress to ε_p=$\varepsilon_{p,0}$+$\Delta\varepsilon_p$.

EXPERIMENTAL INVESTIGATION - TEST SETUP

The test setup is presented in Figures 10 and 11. The girders were both simply supported with a total span of 18 m. In the central third, 4 actuators at a distance of 1.2 m applied point loads (strip loads in transverse direction) under displacement control at a velocity of 1 mm/min for the preloading stage and subsequently 3.5 mm/min for the final failure test. The loading configuration was chosen according to the Polish code for bridge design (PN-85/S-10030 1986). Several LVDTs and strain gauges were installed in order to measure local displacements and strains, locations are given in Figure 11. Concrete compressive strain on top of the girder was measured at five locations along the girder, each time with two strain gauges over the width (SG2.1 and SG2.2 to SG6.1 and 6.2, respectively). For Girder 2, tensile strain of both CFRP strips were recorded at the same location as the corresponding compressive strains on top, in this case one gauge per strip (CFRP2.1,CFRP2.2 to CFRP6.1,CFRP6.2). During the prestressing, two additional gauges per strip (CFRP10.1 and 10.2 and CFRP20.1 and 20.2, respectively) were mounted in order to assess the prestrain $\varepsilon_{fp,0}$ (see Figure 11). Finally, vertical deflections were recorded for both girders at midspan.

RESULTS AND DISCUSSION

Force-deflection

The key results of the tests are summarized in Table 3. The force-midspan deflection curves (only one loading force is plotted, see Figure 11) for both girders are given in Figure 12, and crack pattern after test end for both Girders 1 and 2 are presented in Figure 13. Both girders exhibited shear cracks after a certain load level, but eventually failed in flexure. It can be observed in Figure 12 that prestressing the CFRP strips implicates an increase in the cracking load F_{cr} from about 95 kN for the reference girder to 110 kN for the strengthened structure, corresponding to a relative enhancement of 16%. With a continuously increasing load, the overall structural behavior of the strengthened Girder 2 is as expected clearly stiffer than the reference test. For instance, an increase in bending stiffness from about 746 kN/m for the reference girder to 983 kN/m for the strengthened member can be noticed. Since no strain gauges were used to assess the steel cable strain, the yielding load F_y cannot be determined exactly. Nevertheless, it becomes obvious from the loading curve that the strengthened girder exhibits a higher yielding load (Figure 12). The reference test was conducted up to a deflection δ_u of 260 mm and stopped because of stroke limitation. The increase in load towards the end was extremely small, leading to the conjecture that the reached force F of 193 kN corresponds approximately to the reference ultimate load carrying capacity. For Girder 2, an ultimate load carrying capacity of 240 kN, corresponding to a relative increase of 24% compared to the reference girder, was measured. At that stage, the ultimate tensile capacity of the CFRP strips was reached.

Strain analysis and crack distribution

At the moment of the test end of Girder 1, the ultimate concrete strain in compression ε_c at midspan was 0.23 %. With a sufficient stroke, concrete crushing could be most likely reached. For the strengthened Girder 2, the ultimate load carrying capacity of 240 kN by tensile failure of the CFRP strips was reached at a concrete compressive strain level at midspan of about 0.15%. For both girders, all measured concrete strains plotted against the load F is shown in Figure 14. The previously explained stiffer structural behavior of the strengthened girder is also visible in the strain behavior. It is important to notice that, for both the reference and the strengthened girders, the strain gauges used for capturing the compressive strains on top were mounted after the cable and CFRP strip prestressing. This implicates that the measured and presented values for ε_c in Figure 14 also include a negative concrete strain in tension on the deck side prior to the static loading, and are hence not exactly to be compared with the calculations. The different CFRP tensile strains ε_f evolution in function of the load F are presented in Figure 15a. As mentioned, failure in Girder 2 was eventually obtained by tensile failure in the CFRP strip, measured with a maximal CFRP strain in tension $\varepsilon_{f,u}$ of 1.58% shortly before failure. A photo of the CFRP strips after test end with the carbon filaments is given in Figure 15b. The first flexural crack appeared in the central part in the region of the maximum moments, hence strain gauges on the CFRP strips at the locations x=7800, 8990, and 9000 mm indicate a first stiffness loss at the previously mentioned cracking load F_{cr} of 110 kN (Figure 15). Afterwards, flexural and shear cracks gradually move towards the supports. Strain gauges CFRP10.1 and 10.2 for instance start deviating from the linear elastic region at a load slightly higher than 150 kN. Eventually, cracks reach the area located 3 m from the supports at a force level higher than 210 kN (Figure 15 a)). CFRP tensile strain evolution distributed over half the girder length are given in Figure 16. From the initial prestrain $\varepsilon_{fp,0}$, it was possible to obtain a total strain increase in tension $\Delta\varepsilon_f$ of 1.0% at midspan.

Failure mode

The most important information to be retained from the tests is the tensile failure of the CFRP strips. As mentioned in the introduction, the most inconvenient aspect of initially unstressed and externally bonded composite reinforcement in concrete retrofitting is mostly the fact that the materials' excellent mechanical performance in tension is rather badly exploited to due a premature strip debonding. Also for prestressed strips, debonding is the most common failure mode. In this case, it was possible to fully use the tensile capacity and hence to obtain the highest strengthening level possible. The static system with a large span of 18 m implicated that both anchorage zones were kept apart by around 15 m, possibly having the effect of avoiding a premature debonding as for instance observed with short span beams in (Aram et al. 2008). Additionally, one strong contribution to the overall load carrying capacity might have been the presence of the CFRP wraps for the shear strengthening. Since they were installed after having applied the flexural strengthening, they completely are wrapped around the strip and hence represent a barrier to a premature debonding. This observation is a strong argument in favor of such a shear reinforcement, even when not necessary from a design point of view for shear, since it might strongly improve the overall structural behavior in bending. A further reason for the CFRP tensile failure was also the fact that anchorage zone remained uncracked at the bottom side.

Structural ductility

In Section 5, a strengthening efficiency of 24% when comparing the ultimate load of the strengthened girder (240 kN) to the maximal force of the reference beam (193 kN) was presented. From a structural design point of view, it is also necessary to consider a few ductility aspects for Girder 2. Three ductility index calculations in terms of curvature, deflection at midspan, and energy dissipation are discussed and evaluated for the retrofitted structure.

Since at midspan both the upper concrete strain in compression as well as the CFRP strain in tension are available (measurements), it is possible to determine the curvature at several loading steps. By applying the rule of proportion (sections remain plane), a curvature at steel yielding χ_y of $3.131 \cdot 10^{-6}$ (1/mm) can be obtained for the lowest cable positions at midspan. At failure, the corresponding curvature χ_u is equal to $9.178 \cdot 10^{-6}$ (1/mm). The curvature ductility index μ_χ is equivalent to the ratio between both curvature at failure and at yielding (Eq. 1):

$$\mu\chi = \frac{\chi_u}{\chi_y} \qquad (1)$$

The respective subscripts y and u represent the characteristic values at yielding and ultimate state, respectively. In this case, the index takes the value of 2.93 and thus higher than the minimum value of 2.6 required by the (fib bulletin14 2001) for concrete types higher than C35/45. At failure, an additional steel strain in the cables $\Delta\varepsilon_p$ of 0.93% can be calculated. This value is for instance higher than the requested 0.5% steel strain at failure for conventional reinforcement in a RC element strengthened with an unstressed EBR CFRP strip requested by the (ACI440.2R-8 2008). To summarize, retrofitted Girder 2 satisfies common design requirements. It is noteworthy to mention that the observed additional tensile strain $\Delta\varepsilon_f$ of 1.0% in the CFRP strips at failure is far higher than the ultimately tolerated value of 0.8% for instance by the (SIA166 2004) given for initially unstressed strips.

The classic deformability index μ_δ relates the deflection at failure to the one at steel yielding (Eq. 2):

$$\mu_\delta = \frac{\delta_u}{\delta_y} \tag{2}$$

For Girder 2, the deformability index takes the value 2.1 (see Table 3). Even though the value is smaller than the one comparing the respective curvatures, a clear increase between the midspan displacement at yielding and the one at ultimate load can be noticed.

Numerical parameter study

Figure 17 shows the force-deflection curves for the static loading test with the retrofitted girder compared to numerical simulations with the previously described CSA. Several prestrain levels $\varepsilon_{fp,0}$ ranging from 0.1, 0.2, 0.3, 0.4, 0.5, and eventually 0.58% were calculated. The simulations for Figure 17 were all carried out until tensile failure of the CFRP strip, assuming for all prestrain levels the same failure type as observed in the experimental test with an initial prestrain of 0.58%. Additionally, a limitation for the ultimate load carrying capacity defined by a maximum additional strip strain in tension $\Delta\varepsilon_{fp}$ of 0.8%, as for instance given by the (SIA166

2004), is indicated. It is important to notice that the 0.8% represents an additional strain value to the initial prestrain value $\varepsilon_{fp,0}$. In general, a good agreement between the experimental and numerical curves for an identical strip prestrain level of 0.58% corresponding to the static loading test can be observed. The effect of a higher CFRP prestrain level on the cracking load is not extremely pronounced, the calculated values range between both experimental values for the reference and the retrofitted girder presented earlier in the manuscript (approximately 90 to 110 kN). Regarding the yielding load, however, an increase with a higher initial prestress level is obvious. The corresponding deflection does not significantly change. Since in the first case, tensile failure of the strip is assumed for all calculated scenarios, ultimate load is identical. A gain in structural stiffness after cracking goes together with a reduced ductility in terms of deflection at failure when a higher prestrain level is applied. In this case, the deformability index decreases with a growing CFRP prestrain. These observations are in agreement with classic prestressed concrete theory and technique. When simulating with the above mentioned 0.8%-maximum strip strain as debonding criterion, ultimate load carrying capacity is reached at the same deflection level regardless of the initial strip prestrain. However, a higher value of the latter implicates a higher ultimate bearing capacity. Steel yielding is reached in all the simulated cases. Eventually, contrary to the CFRP tensile failure criterion, it is interesting to notice that the previsously discussed deformability index μ_δ is not affected when the 0.8% criterion is used.

CONCLUSIONS

This paper presents an application of a strengthening method together with an experimental demonstration of its structural efficiency. Several conclusions can be drawn from the results:

- For practical applications, dry shotcrete seems to be a feasible solution for levelling an initially cambered beam or girder in case an additional (C)FRP strip reinforcement has to be installed. The application requires qualified operators, but exhibits good results in terms of bond to the concrete substrate. Even though certain preparation works (for instance a lateral formwork prior to the shotcrete application) are necessary, the overall application time is fast.
- The feasibility of the application of the prestressed CFRP strips with gradient anchorage was proven in the present case. However, additional investigation about the applicability on narrow girder geometries and such dense reinforcement configuration in the bottom flange is necessary.
- For the present case, flexural strengthening by means of prestressed CFRP strips resulted in a clear enhancement of the cracking, yielding, and ultimate load compared to the unstrengthened girder of 16, 19, and 24%, respectively. Additionally, ductility of the structure up to failure was guaranteed.
- The ultimate load of the retrofitted structure was eventually reached by tensile failure of the CFRP strip. The fact of having avoided a CFRP strip debonding indicates a sufficient bond of the total CFRP/epoxy/shotcrete/concrete system good material exploitation of the strips in this case.
- The listed positive aspects of this strengthening and subsequent static testing activities lead to the conclusion that the suggested retrofitting technique by prestressed composite laminates might be a useful and efficient method to

strengthen deficient structural concrete elements in future.

- The key factor is firstly the strengthening efficiency in terms of load carrying capacity. Afterwards, it has to be demonstrated that the retrofitted structure exhibits sufficient ductility, such as for instance required by the (fib bulletin14 2001). The presented verification regarding the curvature ratio of the cross-section at ultimate and steel yielding stage seems to be an adequate method, since it guarantees a distinct steel yielding prior to reaching the ultimate load carrying capacity. This verification is recommended by the authors.

ACKNOWLEDGEMENTS

The presented research is part of the joined multidisciplinary research project TULCOEMPA between Łódź University of Technology and Empa. The financial support of the Polish-Swiss Research Programme for the project PSRP-124/2010 is highly appreciated. The companies S&P Clever Reinforcement Company, S&P Polska, and Granjet Granella AG are kindly acknowledged for their support in the preparation of the concrete elements and material provision. Detailed product information on the composite reinforcements can be found in the respective data sheets (S&P-Clever-Reinforcement-Company-AG 2013d),(S&P-Clever-Reinforcement-Company-AG 2013c),(S&P-Clever-Reinforcement-Company-AG 2013a),(S&P-Clever-Reinforcement-Company-AG 2013b). The help of the laboratory staff of Empa for the testing activities and the image correlation measurements is deeply appreciated.

REFERENCES

ACI440.2R-8 (2008). *Guide for the Design and Construction of Externally Bonded FRP Systems for Strengthening Concrete Structures*. American Concrete Institute.

Aram, M., Czaderski, C., and Motavalli, M. (2008). "Effects of Gradually Anchored Prestressed CFRP Strips bonded on Prestressed Concrete Beams." *Journal of Composites for Construction (ASCE)*, 12(1), 25–34.

Bae, S.-W. and Belarbi, A. (2013). "Behavior of Various Anchorage Systems Used for Shear Strengthening of Concrete Structures with Externally Bonded FRP Sheets." *Journal of Bridge Engineering (ASCE)*, 18(9), 837–847.

Bakis, C., Bank, L., Brown, V., Cosenza, E., Davalos, J., Lesko, J., Machida, A., Rizkalla, S., and Triantafillou, T. (2002). "Fiber-Reinforced Polymer Composites for Construction - State-of-the-art Review." *Journal of Composites for Construction (ASCE)*, 6(2), 73–87.

Berset, T., Schwegler, G., and Trausch, L. (2002). "Verstärkung einer Autobahnbrücke mit vorgespannten CFK-Lamellen." *tec21*, 128(22), 22–29.

Blaschko, M. and Zehetmaier, G. (2008). "Strengthening the Röslautal Bridge Using Innovative Techniques, Germany." *Structural Engineering International*, 18(4), 346–350.

Cerullo, D., Sennah, K., Azimi, H., Lam, C., Fam, A., and Tharmabala, B. (2013). "Experimental Study on Full-Scale Prestrensioned Bridge Girder Damaged by Vehicle Impact and Repaired with Fiber-Reinforced Polymer Technology." *Journal of Composites for Construction (ASCE)*, 17(5), 662–672.

Czaderski, C., Martinelli, E., Michels, J., and Motavalli, M. (2012). "Effect of Curing Conditions on Strength Development in an Epoxy Resin for Structural Strengthening." *Composites Part B: Engineering*, 43(2), 398–410.

DAfStb (2012). *Guideline: Strengthening of concrete members with adhesively bonded reinforcement - Part 1*. Deutscher Ausschuss für Stahlbeton, 120 pages.

DIN-EN-ISO-527-5 (1997). *Plastics - Determination of tensile properties - Part 5: Test conditions for unidirectional fibre-reinforced plastics (German Version)*. Deutsches Institut für Normung (DIN), 8 pages.

El-Hacha, R., Wight, R., and Green, M. (2001). "Prestressed Fibre-Reinforced Polymer Laminates for Strengthening Structures." *Progress in Structural Engineering and Materials*, 3, 111–121.

El-Hacha, R., Wight, R., and Green, M. (2003). "Innovative System for Prestressing Fiber-Reinforced Polymer Sheets." *ACI Structural Journal*, 100(3), 305–313.

fib bulletin14 (2001). *Externally bonded FRP reinforcement for RC structures*. International federation for structural concrete, 130 pages.

Harmanci, Y. (2013). *Prestressed CFRP for Structural Retrofitting - Experimental and Analytical Investigation*. M.Sc. thesis, ETH Zürich.

Hognestad, E. (1951). *A study of combined bending and axial load in reinforced concrete members*. Bulletin 399, pp.129. University of Illinois Engineering Experimental Station.

Kasan, J., Harries, K., , Miller, R., and Brinkman, R. (2014). "Repair of Prestressed-Concrete Girders Combining Internal Strand Splicing and Externally Bonded CFRP Techniques." *Journal of Bridge Engineering (ASCE)*, 19(2), 200–209.

Kim, Y., Green, M., and Fallis, G. (2008). "Repair of Bridge Girder damaged by Impact Loads with Prestressed CFRP sheets." *Journal of Bridge Engineering*

(ASCE), 13(1), 15–23.

Kotynia, R., Walendziak, R., Stöcklin, I., and Meier, U. (2011). "RC Slabs strengthened with Prestressed and Gradually Anchored CFRP Strips under Monotonic and Cyclic Loading." *Journal of Composites for Construction (ASCE)*, 15(2), 168–180.

Meier, U. (1995). "Strengthening of structures using carbon fibre/epoxy composites." *Construction and Building Materials*, 9(6), 341–351.

Meier, U. and Stöcklin, I. (2005). "A Novel Carbon Fiber reinforced Polymer (CFRP) System for Post-Strengthening." *International Conference on Concrete Repair, Rehabilitation and Retrofitting (ICCRRR)*, Cape Town, South Africa.

Meier, U., Stöcklin, I., and Terrasi, G. (2001). "Civil engineers can make better use of the strength of fibrous materials." *International Conference on Composites in Construction (CCC)*, Porto, Portugal.

Michels, J., Sena-Cruz, J., Czaderski, C., and Motavalli, M. (2013). "Structural Strengthening with Prestressed CFRP Strips Anchored with the Gradient Method." *Journal of Composites for Construction (ASCE)*, 17(5), 651–661.

Michels, J., Staskiewicz, M., Czaderski, C., Lasek, K., Kotynia, R., and Motavalli, M. (2014). "Anchorage resistance of CFRP strips externally bonded to various cementitious substrates." *Composites Part B: Engineering*, 63, 50–60.

Park, R. and Paulay, T. (1975). *Reinforced Concrete Structures*. Bulletin 399, pp.129. John Wiley & Sons.

Pellegrino, C. and Modena, C. (2009). "Flexural Strengthening of real-scale RC and PRC Beams with End-anchored Pretensioned FRP Laminates." *ACI Structural Journal*, 106(3), 319–328.

Petrou, M., Parler, D., Harries, K., and Rizos, D. (2008). "Strengthening of Reinforced Concrete Bridge Deck using Carbon Fiber-Reinforced Polymer Composite Materials." *Journal of Bridge Engineering (ASCE)*, 13(5), 455–467.

PN-85/S-10030 (1986). *Bridges - Loads*. Polski komitet normalizaciji, miar i jakoci.

PN-91/S-10042 (1991). *Bridges - Concrete structures, reinforced and prestressed - Design*. Polski komitet normalizaciji, miar i jakoci, 33 pages.

Puurula, A., Enochsson, O., Sas, G., Blanksvärd, T., Ohlsson, U., Bernspang, L., Täljsten, B., Carolin, A., Paulsson, B., and Elfgren, L. (2014). "Assessment of the Strengthening of an RC Railway Bridge with CFRP Utilizing Full-Scale Failure Test and Finite-Element Analysis." *Journal of Structural Engineering (ASCE)*, DOI:10.1061/(ASCE)ST.1943-541X.0001116.

SIA166 (2004). *Klebebewehrungen (Externally Bonded Reinforcement)*. Schweizer Ingenieur- und Architektenverein, Switzerland, 44 pages.

S&P-Clever-Reinforcement-Company-AG (2013a). *S&P 50/55 epoxy adhesive - Technical data sheet*. S&P Clever Reinforcement Company AG, available under www.reinforcement.ch.

S&P-Clever-Reinforcement-Company-AG (2013b). *S&P C-sheet 240 - Technical data sheet*. S&P Clever Reinforcement Company AG, available under www.reinforcement.ch.

S&P-Clever-Reinforcement-Company-AG (2013c). *S&P Laminates CFK - Technical data sheet*. S&P Clever Reinforcement Company AG, available under www.reinforcement.ch.

S&P-Clever-Reinforcement-Company-AG (2013d). *S&P Resin 220 epoxy adhesive -*

Technical data sheet. S&P Clever Reinforcement Company AG, available under www.reinforcement.ch.

Suter, R. and Jungo, D. (2001). “Vorgespannte CFK-Lamellen zur Verstärkung von Bauwerken.” *Beton- und Stahlbetonbau*, 96(5), 350–358.

Wight, R., Green, M., and Erki, M.-A. (2001). “Prestressed FRP Sheets for Post-strengthening Reinforced Concrete Beams.” *Journal of Composites for Construction (ASCE)*, 5(4), 214–220.

Xue, W., Zeng, L., and Tan, Y. (2008). “Experimental Studies on Bond Behaviour of High Strength CFRP Plates.” *Composites Part B: Engineering*, 39(4), 592–603.

List of Tables

TABLE 1: Concrete compressive strength on cube f_{cm} and elastic modulus E_{cm} at 28 days and at testing day, n.a.=not available

Time	f_{cm} [MPa]	E_{cm} [GPa]	f_{cm} [MPa]	E_{cm} [GPa]
	Girder 1		Plate 1	
28 days	61.4	34.9	47.5	33.3
test day	64.6	34.7	50.0	32.1
	Girder 2		Plate 2	
28 days	62.1	33.5	51.1	34.0
test day	66.9	n.a.	53.5	n.a.

TABLE 2: Yield strength, tensile strength and strain at failure of the passive steel bar reinforcement without ribs

Ø [mm]	R_i [MPa]	R_m [MPa]	$\varepsilon_{s,u}$ [%]
6	387	485	15.3
8	462	545	10.6

TABLE 3: Key results of the static girder tests

Parameter	Girder 1	Girder 2
δ_{cr} [mm]	22	23
F_{cr} [kN]	95	110
δ_y [mm]	100	100
F_y [kN]	160	190
δ_u [mm]	260	208
F_u [kN]	193	240
$\varepsilon_{c,max}$ [%]	0.23	0.15
$\varepsilon_{f,max}$ [%]	-	1.58
Failure mode	Towards concrete crushing	CFRP tensile failure

List of Figures

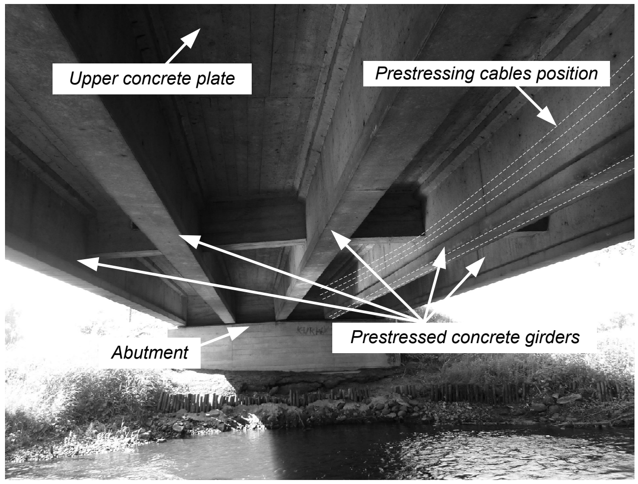

FIG. 1: Bottom view of the road bridge in Poland before retrofitting (image by Julien Michels)

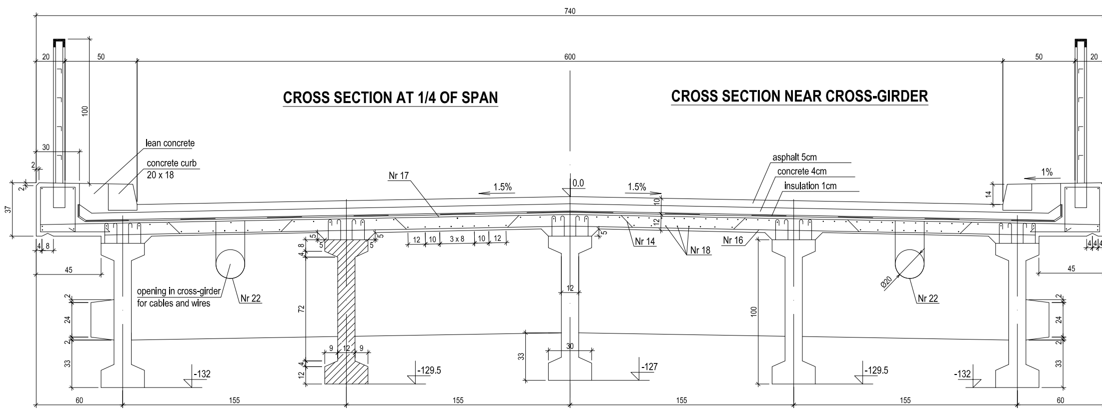

FIG. 2: Bridge cross section before retrofitting (dimensions in [cm])

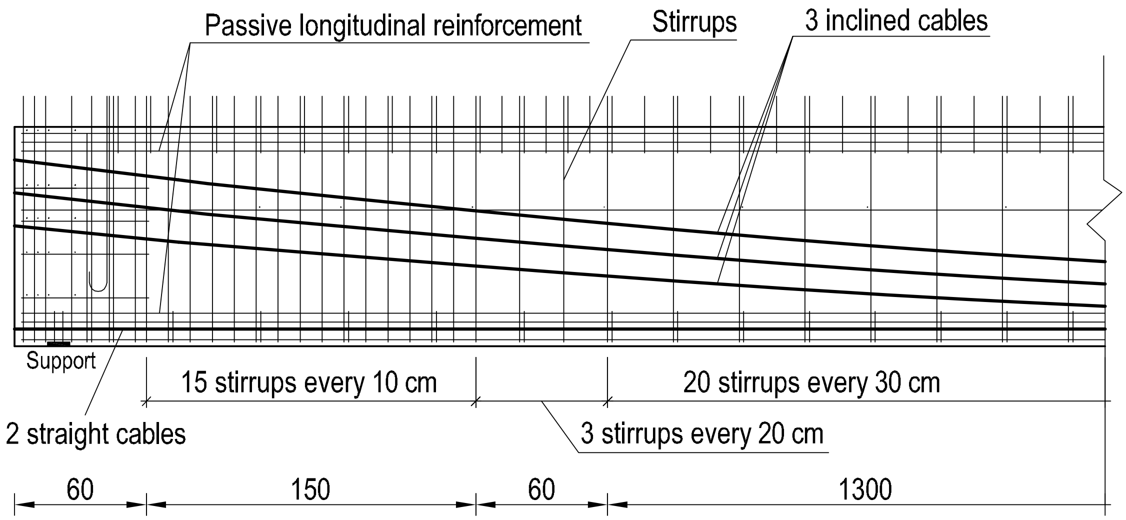

FIG. 3: Extract of flexural (passive and prestressed) and shear reinforcement over a part of the girder length (without the upper slab)

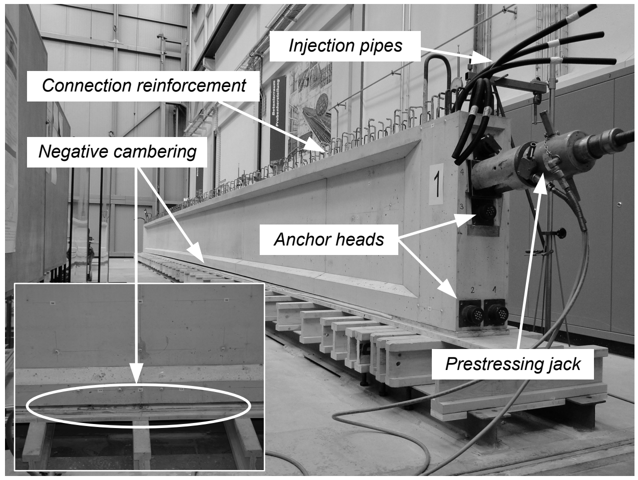

FIG. 4: Casting and prestressing of the prestressed concrete girder(s) (images by Julien Michels)

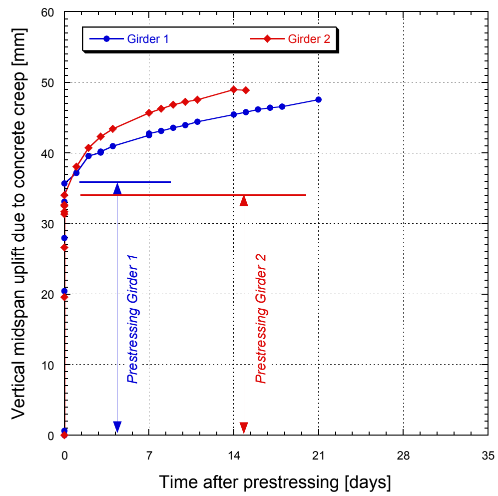

FIG. 5: Vertical displacement at midspan due to prestressing and concrete creep over time

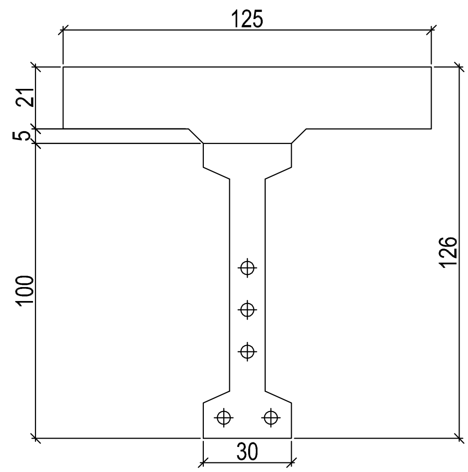

FIG. 6: Cross-section of the casted girder (dimensions in [cm])

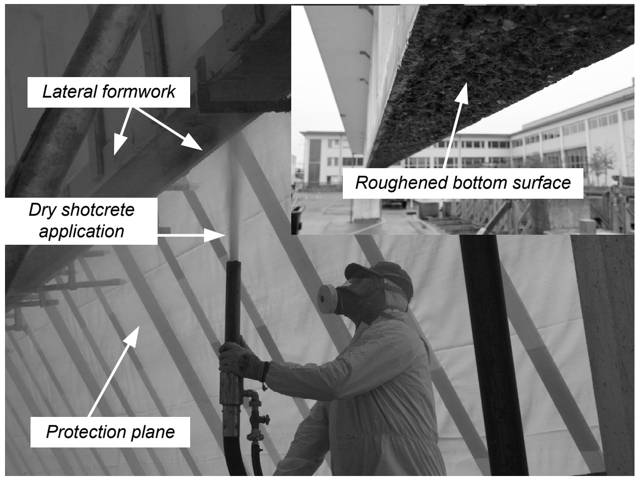

FIG. 7: Roughened bottom surface after waterjetting at high pressure and dry shotcrete application (images by Julien Michels)

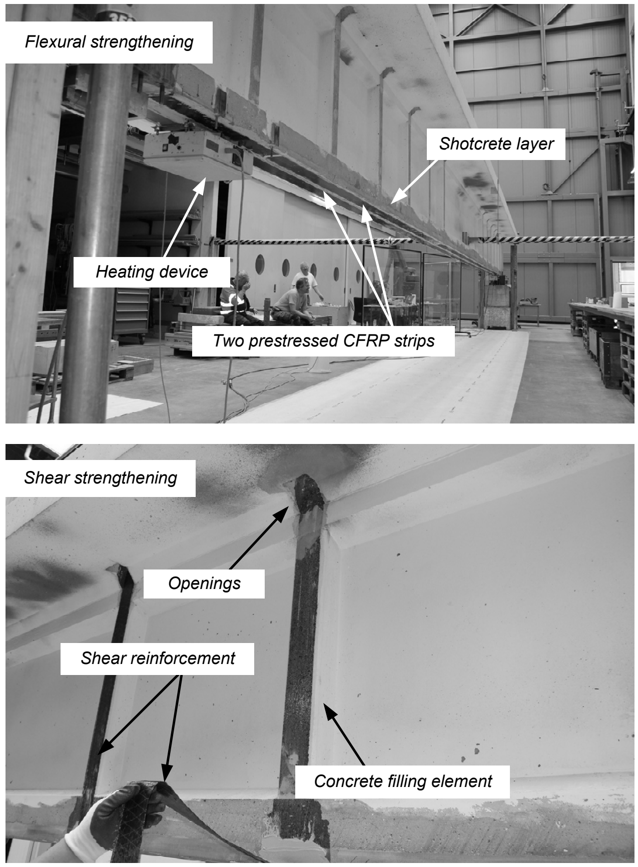

FIG. 8: Flexural and shear reinforcement for the large scale girder (images by Julien Michels)

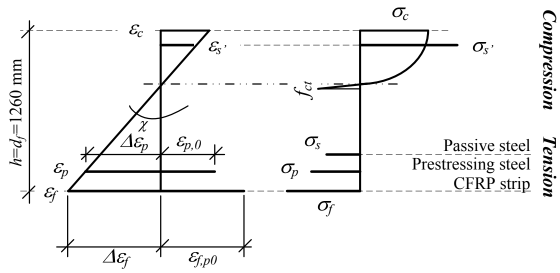

FIG. 9: Cross-section analysis (CSA) - inidication of the strain state at the moment of CFRP prestressing and anchoring

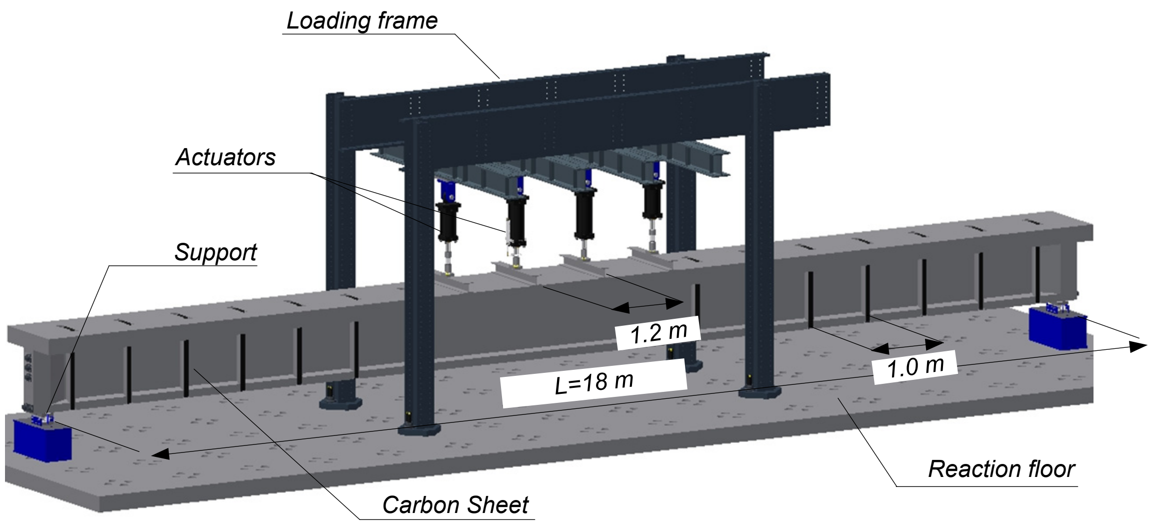

FIG. 10: Test setup for the large-scale static tests

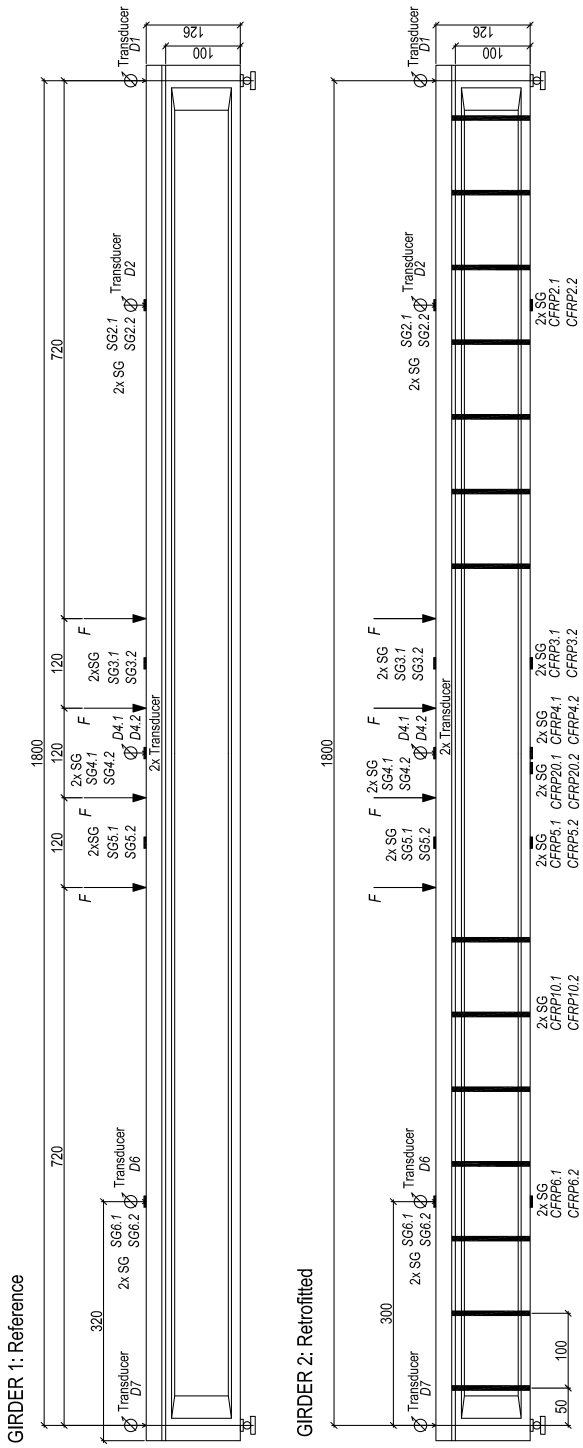

FIG. 11: Measurements configuration (dimensions in [cm])

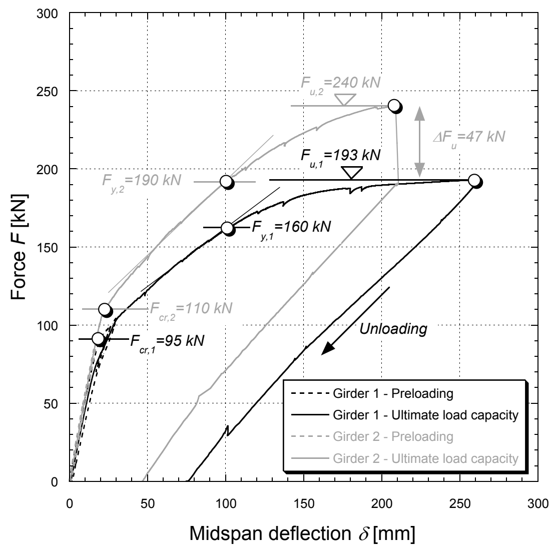

FIG. 12: Force-deflection (midspan) curves of Girder 1 and 2 up to the ultimate load carrying capacity

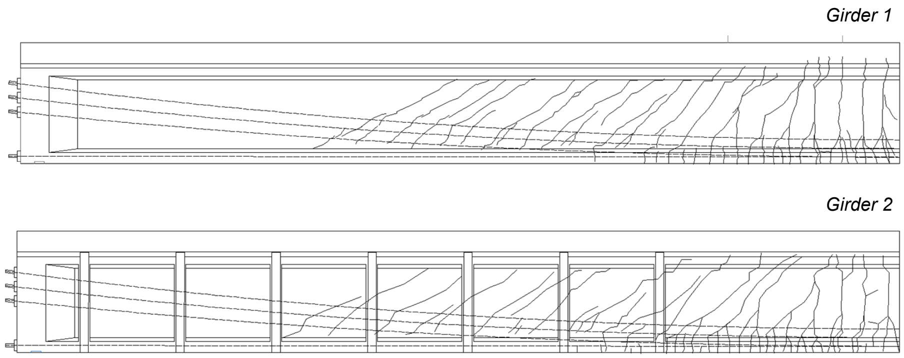

FIG. 13: Final crack pattern after test end (support to midspan)

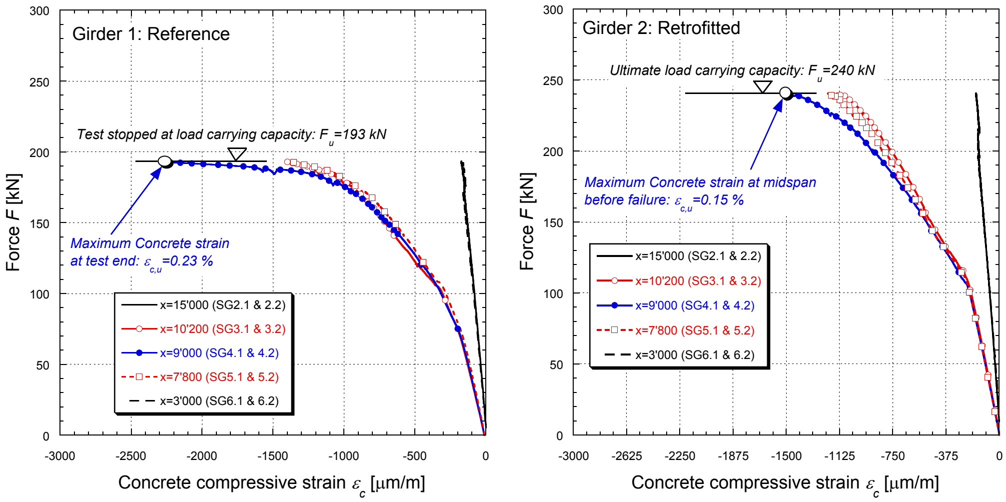

(a) F-ε_c for Girder 1 (b) F-ε_c for Girder 2

FIG. 14: Force-compressive concrete strain at midspan for both Girders 1 and 2

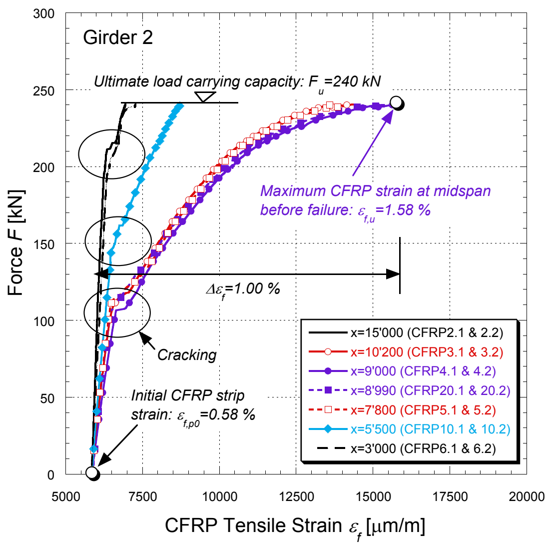

(a) F-ε_f for Girder 2

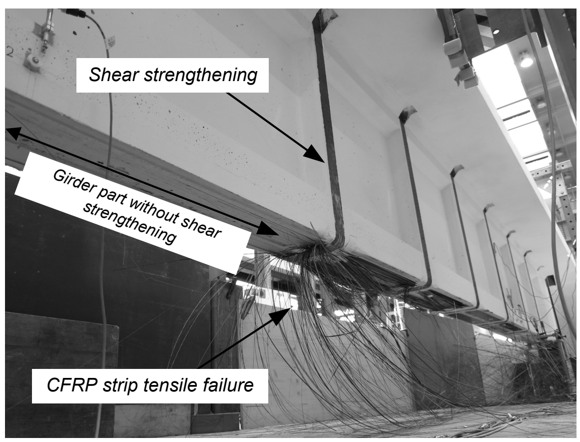

(b) CFRP strips after tensile failure

FIG. 15: Force-CFRP tensile strain (F,ε_f) diagram and photo of the CFRP strips after tensile failure (image by Julien Michels)

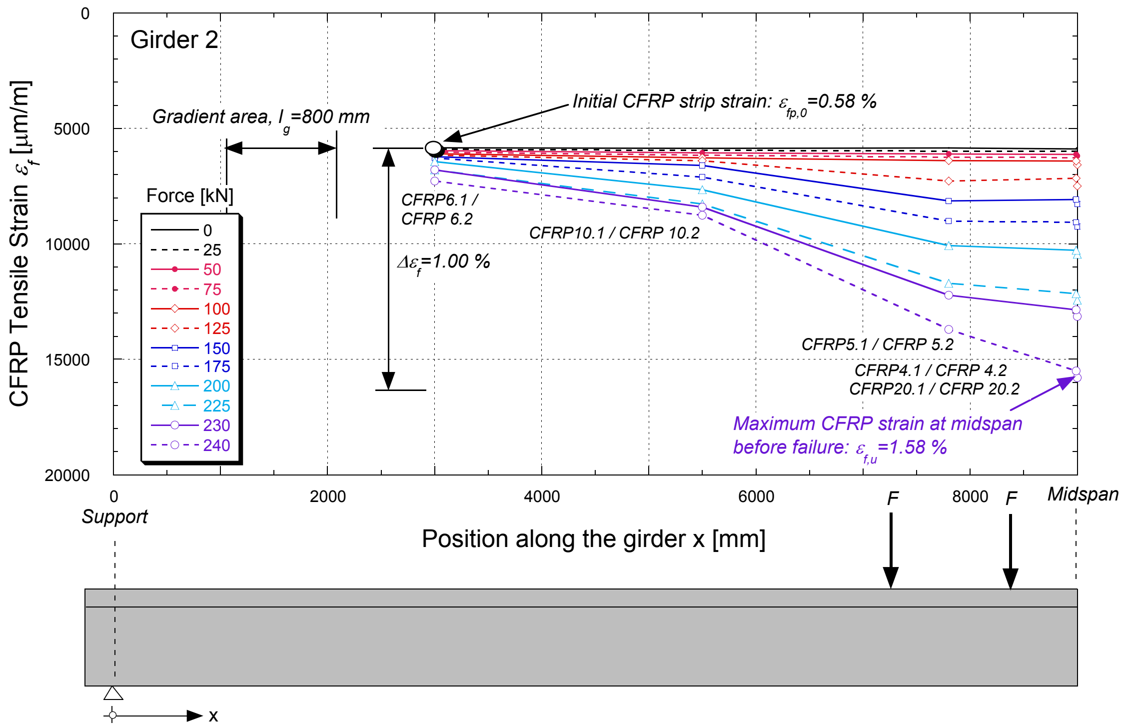

FIG. 16: CFRP tensile strains ε_f (including the prestrain $\varepsilon_{fp,0}$=0.58%) evolution over the horizontal girder axis with growing load in [kN] (axis not in scale)

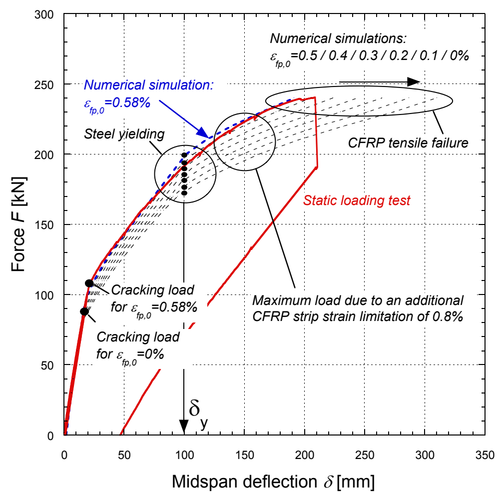

FIG. 17: Numerical simulations with various prestrain levels $\varepsilon_{fp,0}$